Atmos. Chem. Phys. Discuss., 3, 3051–3094, 2003
www.atmos-chem-phys.org/acpd/3/3051/

Atmospheric Chemistry and Physics Discussions

Transport and build-up of tropospheric trace gases during the MINOS campaign: Comparision of GOME, in situ aircraft measurements and MATCH-MPIC-data

A. Ladstätter-Weißenmayer[1], J. Heland[2], R. Kormann[3], R. v. Kuhlmann[3], M. G. Lawrence[3], J. Meyer-Arnek[1], A. Richter[1], F. Wittrock[1], H. Ziereis[3], and J. P. Burrows[1]

[1]Institute of Environmental Physics, University of Bremen, P.O. Box 330440, D-28334 Bremen, Germany
[2]Institute of Atmospheric Physic, DLR, Oberpfaffenhofen, D-82234 Wessling, Germany
[3]Max-Planck-Institute for Chemistry, P.O. Box 3060, D-55020 Mainz, Germany

Received: 4 March 2003 – Accepted: 15 May 2003 – Published: 5 June 2003

Correspondence to: A. Ladstätter-Weißenmayer (lad@iup.physik.uni-bremen.de)

Abstract

The MINOS (Mediterranean INtensive Oxidant Study) campaign was an international, multi-platform field campaign to measure long-range transport of air-pollution and aerosols from South East Asia and Europe towards the Mediterranean basin during August 2001. High pollution events were observed during this campaign. For the Mediterranean region enhanced tropospheric nitrogen dioxide (NO_2) and formaldehyde (HCHO), which are precursors of tropospheric ozone (O_3), were detected by the satellite based GOME (Global Ozone Monitoring Experiment) instrument and compared with air-borne in-situ-measurements as well as with the output from the global 3D photochemistry-transport model MATCH-MPIC (Model of Atmospheric Transport and CHemistry – Max-Planck-Institute for Chemistry). The increase of pollution in that region leads to severe air quality degradation with regional and global implications.

1. Introduction

The rapid growth of human population and industrial development in South-East Asia and Europe is accompanied by an increase of air pollution. The consequence is increasing trace gases production and released into the atmosphere by human activities which are significantly disturbing the composition and chemistry of the global atmosphere and increasing the concentration of atmospheric greenhouse gases that control the climate of our planet (Levine, 1991). Combustion processes lead to emissions of trace gases like carbondioxide (CO_2), carbon monoxide (CO), nitrogenoxide (NO_x) [NO_x = NO+NO_2], methane (CH_4), nonmethane hydrocarbons (NMHC) and especially formaldehyde (HCHO) which is also produced by photochemical reactions (Ladstätter-Weißenmayer et al. 1998). These reactive gases strongly influence the local and downwind concentrations of the major oxidant ozone (O_3).

Here we evaluated measurements of the Mediterranean INtensive Oxidant Study 2001 campaign to characterize the atmospheric chemical composition of SE-Asian

ACPD

3, 3051–3094, 2003

and European outflow from July and August 2001 during the biomass burning season over the Mediterranean basin. This season was selected because northeasterly winds are persistent during this period and convection over the continental source regions is suppressed by large-scale subsidences, thus limiting the upward dispersion of pollution. As part of this MINOS campaign the Department of Environmental Physics and Remote Sensing (IUP), University of Bremen, Germany, analysed satellite based GOME data to compare the results to in-situ aircraft measurements of the trace gases NO_2 (Heland et al., 2002). In addition for the first time the comparisons between in-situ aircraft and GOME data were carried out for the trace gas formaldehyde (HCHO) (Ladstätter-Weißenmayer et al. 1998; Chance et al. 2000; Palmer et al. 2002) on both a regional and a global scale to investigate transportation and build-up of tropospheric pollution over the Mediterranean basin.

The vertical columns of HCHO were determined directly from the GOME data. For the NO_2 retrieval the Tropospheric Excess Method (Richter et al., 2002; Leue et al., 2001) was used to separate tropospheric and stratospheric amounts. The results were compared with those from the in-situ aircraft profile measurements of NO_2 (performed by the Institute of Atmospheric Physics, DLR (Deutsches Zentrum für Luft- und Raumfahrt), Oberpfaffenhofen) and of HCHO (provided by the Max Planck Institute for Chemistry, Mainz) as well as with simulations from the MATCH-MPIC-model, operated by the Max Planck Institute for Chemistry, Mainz (v. Kuhlmann, 2001; v. Kuhlmann et al., 2002; Lawrence et al., 1999).

2. Experimental setup

2.1. GOME measurements

GOME was launched in April 1995 onboard the European Research Satellite (ERS)-2 into a near-sun-synchronous orbit at a mean altitude of 795 km. The descending mode crosses the equator every 2800 km at 10:30 am local time. GOME is a nadir-

ACPD
3, 3051–3094, 2003

scanning double-monochromator measuring the sunlight scattered from Earth's atmosphere and/or reflected by the surface in the wavelength region of 240 to 790 nm at a moderate spectral resolution of 0.17 to 0.33 nm. Once per day the extraterrestrial solar irradiance is measured and can be used as an absorption free background in the data analysis. The spectrum is subdivided into four spectral channels, each recorded quasi-simultaneously by a 1024-pixel reticon photodiode-array. With 14 orbits per day, total ground coverage is obtained within 3 days at the equator by a 960 km across-track swath (4.5 s forward scan, 1.5 s back scan, the size of one GOME ground pixel is $40 \times 320\,km^2$). GOME measurements are available since July 1995. The main scientific objective of GOME is to measure the global distribution of O_3 and several other trace gases which play an important role in the ozone chemistry of the Earth's stratosphere and troposphere, e.g. NO_2, BrO, OClO, SO_2 and HCHO. Details of the overall scientific results are reported elsewhere (Burrows et al., 1999; Burrows et al., 2000).

During the summer in the boundary layer (BL) over the Mediterraen region the mixing ratios for NO_2 are normally in a range of 0.2–0.7 ppb (measured by M. Vrekoussis with a long-path DOAS (Differential Optical Absorption Spectroscopy)-system during the MINOS campaign) near the surface. For HCHO a mixing ratio of 200 ± 70 ppt was measured during the INDOEX-campaign (Wagner et al., 2002) in the marine boundary layer over the Indian Ocean, whereas an average value of 1.6 ppb could be observed during the MINOS campaign (Kormann et al., 2003). GOME is able to measure both trace gases with a detection limit of $5 \cdot 10^{14}$ molec/cm^2 (~100 ppt, considering a 2 km thick atmospheric layer at 1000 hPa) for NO_2 and $2.5 \cdot 10^{15}$ molec/cm^2 (~500 ppt, considering a 2 km atmospheric layer at 1000 hPa) for HCHO.

Since GOME is measuring the sunlight backscattered from the earth surface, the presence of clouds influences the results of the data analysis. For this study only GOME measurements under clear sky conditions (with a cloud-cover less than 10%, see Fig. 1a/b, white gaps reflect pixels with cloud cover higer thn 10%) at a spatial resolution of $960 \times 40\,km^2$ (each pixel $320 \times 40\,km^2$) were used for the comparisons with in-situ measurements and modeled MATCH-MPIC-data (Lawrence et al. 2002). The

number of the overflights of GOME over this region during the MINOS campaign and the limitation of cloud-cover determined the factor for the frequency of comparisions.

2.2. Airborne in situ measurements

In-situ measurements of nitrogen monoxide (NO), O_3, HCHO, the photolysis frequency of NO_2 ($J(NO_2)$) and meteorological parameters were performed with the Falcon research aircraft of DLR. NO was measured by means of a well characterized chemiluminescence detector (CLD) with a detection limit of about 5 pptV for NO. The nominal accuracy of the measurements during the MINOS campaign was 5% (Ziereis et al., 1999). Before every flight a calibration of this instrument was performed using a diluted mixture of 2.97 ppmV ±1% NO in N_2 (Messer Griesheim) with purified air.

O_3 was measured by UV-absorption with a modified TE 49 instrument (Thermo Environmental) calibrated with an O_3 41M ozone generator (ANSYCO) which is frequently calibrated against a GAW (Global Atmosphere Watch) standard device. The accuracy of the ozone measurements is estimated to be within 5%.

The photolysis frequency of NO_2 was obtained from the sum of two filter radiometers (Meteo Consult GmbH) (Junkermann et al., 1989; Volz-Thomas et al., 1996) with 2π viewing geometry with an overall uncertainty of 17%. One of the radiometers was installed on top of the aircraft, the second on the downward facing side of the aircraft body. The detectors were optimized for flight applications (Volz-Thomas et al., 1996) and have recently been characterized in the laboratory (Hauser, 2002).

HCHO measurements during MINOS were based on the Hantzsch reaction technique (Nash, 1953) and carried out with an Aero Laser (AL4021, Aero Laser GmbH, Garmisch-Partenkirchen, Germany) modified for airborne operation. The detection limit of the instrument was 42 pptv at a time resolution of 180 s (10–90%). The total uncertainty of HCHO for the measurements during the MINOS campaign is estimated of 30% at a mixing ratio of 300 pptv (Kormann et al., 2003). Similar measurement techniques are described in literature elsewhere (Kelly et al., 1994; Macdonald et al.,

ACPD
3, 3051–3094, 2003

1999).

2.3. MATCH-MPIC-model

The MATCH-MPIC model (Lawrence et al., 1999) has been developed and applied towards the investigation of global tropospheric chemistry. It is an "offline" model which can be driven with gridded time-dependent values from different meteorological datasets. Here, the National Center for Environmental Prediction (NCEP), GFS (Global Forecast/Analysis System), – formerly known as "AVN" – data at a horizontal resolution of about 2.8° × 2.8° with 42 levels are used for the period of the MINOS campaign (Lawrence et al., 2002). Emissions of 16 species from industrial activities (based on the EDGAR database, Olivier et al., 1996), biomass burning, the terrestrial biosphere itself and the ocean were taken into account. The chemical scheme of the model includes CH_4-CO-HO_x-NO_x "background" chemistry, as well as representations of isoprene, ethane (C_2H_6), propane (C_3H_8), ethylene (C_2H_4), propylene (C_3H_6) and higher alkanes. A complete description of the model can be found in Lawrence et al. (1999), v. Kuhlmann et al. (2001, 2003).

3. Data analysis

3.1. GOME data analysis

For the comparisons with the airborne in-situ measurements GOME data, more precisely those corresponding to the pixels along the flight track of the Falcon, were extracted and analysed (see Fig. 1a/b) for the trace gases HCHO and NO_2 (Heland et al., 2002; Richter et al., 2002). GOME lv1-spectra have been analysed using the IUP Bremen Differential Optical Absorption (DOAS) algorithm (Burrows et al., 1999) to derive slant columns of HCHO and NO_2. Vertical columns have been computed with the radiative transfer model GOMETRAN (Rozanov et al., 1997) by calculating the air

ACPD
3, 3051–3094, 2003

mass factors (AMF) (dividing the observed slant columns by the AMF yields the vertical columns), which depends on the absorption path.

Due to the viewing mode of GOME, the largest contribution of the information is coming from the stratosphere. Assuming that there are only small changes in the longitudinal amounts of stratospheric trace gases near the equatorial region compared to the diurnal latitudinal variability, it is possible to use the trace gase amounts (e.g. for NO_2) in the Atlantic region (315 – 325°) as a relatively clean atmospheric background. Under this assumption, the Tropospheric Excess Method (TEM) (Fishman et al., 1990; Richter and Burrows, 2002) can be used in order to calculate the tropospheric excess of a given trace gas by comparing the spectra acquired over the Atlantic with the data from the Mediterranean. An influence of polluted air masses from South-America on NO_2 can be excluded because of the difference in latitude. The concept of deriving tropospheric excess columns of NO_2 is based on (a) the determination of the total column amount in the measurements along the path downwards to the boundary layer – without limitation in detecting the free and upper troposphere – and (b) the subtraction of the estimated stratospheric columns by using data from a polluted area combined with data from a so called "clean air" region under almost cloud free conditions. The reason for this is that GOME tropospheric columns are only obtained by subtracting the above-cloud stratospheric NO_2 amount from the total NO_2 with a reflectivity of < 0.1. For the determination of the vertical tropospheric column the airmass factor has to be included.

The TEM works under the assumption, that the variations in the vertical columns detected by GOME can be attributed to variations in tropospheric NO_2 columns. There are general limitations using this method. One of these uncertainties is in the correction of the stratosphere that means the elimination of the stratospheric amount and a number of input parameters used for the AMF calculation. A detailed discussion of the error budget is given in Richter and Burrows (2002). The main error sources are the inhomogeneities in the stratospheric NO_2 field, and uncertainties in cloud cover, the assumed vertical profile of NO_2, the surface albedo and the aerosol loading which are

ACPD
3, 3051–3094, 2003

required in calculating the AMF. The overall error of the analysis is estimated to be on the order of 1.5×10^{15} molec/cm^2 (see Table 1). For the comparision with in-situ measurements various AMF based on different vertical NO_2-profiles (the individual and the averaged NO_2-profil) were used for the GOME analyses to determine the tropospheric vertical NO_2 columns. They were computed using in-situ measurements and the different types of aerosols and the presence of clouds in the different layers.

The Mediterranean region exhibits a large variability in tropopause height (Shimizu et al., 2000). Taking into account the profiles of the O_3 in-situ measurements up to a height of 13 km an increase of the concentration was observed at 12 km height most likely originating from an influence of stratospheric air masses at this altitude e.g. on 22 August 2001. Considering additionally a higher atmospheric level the height of the tropopause was defined to be at the altitude of 4 PV-Units for the MINOS campaign (see Fig. 2). Therefore the meteorological data is derived from ECMWF-operational analysis at a $1.5 \times 1.5^{\circ}$ resolution based on 60 layers of the analysis-model. Variations in tropopause height in this range have almost no influence in the tropospheric vertical columns of NO_2 in contrast to O_3 caused by the vertical profiles of these trace gases.

There might be a mismatch in orbital and sampling characteristics between GOME and the airborne measurements and additionally the total NO_2 detected by GOME does not include near-surface NO_2 contributions over surfaces with low albedo with 100% efficiency. HCHO is mainly present in the troposphere, so a separation between stratosphere and troposphere is not necessary and the tropospheric columns of HCHO can be determined directly from the vertical columns of this trace gas. The uncertainty of the GOME columns for tropospheric HCHO is dominated by the calculation of the AMF (see Table 1) and the uncertainty in view to the fitting error (fitting window for HCHO: 335–357 nm in contrast to the fitting window of NO_2: 425–455 nm).

ACPD
3, 3051–3094, 2003

3.2. In-situ airborne data analysis

3.2.1. NO_2

The profiles of the airborne measurements like NO, O_3, HCHO and in addition $J(NO_2)$ were analysed in combination with meteorological data. To obtain the NO_2 concentrations we assumed a simple photochemical equilibrium between NO, NO_2 O_3 and $J(NO_2)$ (e.g. Atkinson, 2000), where the temperature-dependent rate constant $k(NO + O_3)$ is calculated from the data given in Sander et al. (2000). For the purpose of data reduction, the airborne NO_2 and O_3 data (1 Hz values) were averaged in 100 m altitude bins for each profile as well as for an averaged NO_2-profile. The error bars were evaluated from the spread of the experimental data in the bins (1σ) and the uncertainties for the NO_2 and O_3 data, respectively. One of the uncertainties for NO_2 can be caused with respect to the simple photochemical equilibrium used between NO, NO_2 O_3 and JNO_2 and the assumption that O_3 dominates the conversion of NO to NO_2 (Calvert and Stockwell, 1983). In polluted regions reactions involving peroxy radicals may also constitute potentially important conversion channels of NO to NO_2 (Crawford et al., 1996). In addition the temperature-dependent rate constant $k(NO + O_3)$ in the above equation, which is a function of non-linear pressure and temperature, can be considered as an uncertainty in the calculation of NO_2. In case of missing data in intermediate altitude bins a mean mixing ratio was defined within these bins and conservative assumptions about the uncertainties were made.

Since the in-situ data were collected up to altitudes of about 10–13 km the analysis of tropospheric vertical columns of NO_2 can be carried out up to the height of 12 km (strong inceasing of O_3) directly. However, the comparisions of the height of the tropopause (which was found to be range within 15.0 to 17.0 km altitude, based on the ECMWF-data) on some days during the MINOS campaign (see Fig. 2) must be taken into account. So the NO_2 datasets had to be extrapolated up to higher altitudes. The linear extrapolation of the NO_2 mixing ratios towards the tropopause starts with the value at the highest aircraft altitude and ends with the highest measured value of NO_2

ACPD
3, 3051–3094, 2003

in the free troposphere. The error bars for the extrapolated NO_2 mixing ratios were set to be ±100%.

In order to obtain tropospheric columns of NO_2 the number densities of this trace gas in the defined altitude bins were summed up and multiplied with the thickness of the bins, (i.e. 100 m) and finally transfered into molec/cm^3, taking into account the nonlinearity of pressure and temperature. The column uncertainties were calculated using the differences of the minimum or maximum values of the columns – as derived from the error bars – and the mean columns. The overall uncertainty of the nitrogen dioxide mixing ratios depends on the experimental uncertainties of the other gases, i.e. J(NO_2), the reaction constant k, and on the unknown amount of NO_2 produced by molecules other than O_3 (e.g. RO_2) and is estimated to be ~25%.

3.2.2. HCHO

A detailed description of the HCHO data sampling procedure during the MINOS campaign and a disscussion of the data quality is given in Kormann et al. (2003). Data in the lower and middle troposphere (heights of 600 m up to 13 km) were obtained during some profile measurements. These profile measurements contained rapid ascents and descents of the Falcon as well as flights in a constant altitude. For the validation with satellite based data and the intercomparison with the model, calculated profiles from individual flights with a height resolution of 1 km as well as an averaged profile for the campaign were used. Before averaging the data of the HCHO-profiles in bins of 1 km the mixing ratios of HCHO were calculated in molec/cm^3 to consider the non-linearity of pressure and temperature.

3.3. MATCH-MPIC-model-data analysis

The output of the MATCH-MPIC-model is based on data which are interpolated in space and time along the Falcon track (Lawrence et al., 2002). This was done rather than profiles only over Crete, so that the corresponding meteorological conditions for

ACPD
3, 3051–3094, 2003

given temporal and spatial domains were deployed. The profiles of NO_x, NO, O_3, HCHO and in addition J(NO_2) based on MATCH-MPIC-model-output were analysed. To obtain the NO_2 concentrations and eventually the tropospheric vertical columns the same photochemical equlilibrium as described above and as well as the NO_2 calculated from the difference between NO_x and NO were used whereas the HCHO mixing ratios could directly be retrieved from the MATCH-MPIC output. In order to reduce the size of the dataset for NO_2 the values were averaged in 100 m and the output of HCHO in 1 km altitude bins, to be consistent with the in-situ measurements.

4. Results and discussion

The first scientific aim was to calculate the tropospheric amount of the satellite based GOME measurements for NO_2 and HCHO and to compare these results with in-situ aircraft measurements as well as with the output of MATCH-MPIC during the MINOS campaign. The second aim was to interpret these data with the results of the global detected GOME data with respect to the transport and formation of tropospheric trace gases during this campaign.

It was possible to analyse the GOME data along the Falcon track and therefore to observe the build-up of tropospheric trace gases and in addition to track the transport of air masses.

4.1. Comparison of GOME, in-situ aircraft measurements and MATCH-MPIC-data over the Mediterranean region

Figure 3 shows the measured values of NO_2-concentrations (molec/cm^3) and the calculated averaged profile including the extrapolation of these data up to a height of 18 km with an error of ±100%. For HCHO no extrapolation for the measured and the calculated mean value was carried out and the results up to the maximum flight altitude of about 13 km are shown (see Fig. 4).

ACPD
3, 3051–3094, 2003

Due to the limited temporal and spatial overlap of GOME and aircraft data, only the data of 6 days during the MINOS campaign (one flight on 1, 12, 16, 17 and two fligths per day on 14 and 19 August 2001) could be analysed and compared (see Figs. 5 and 6). For 14 and 19 August 2001 daily mean values for the tropospheric columns of NO_2 and HCHO aircraft measurements were used for the comparisons with GOME data.

Analysing the GOME data the following procedure was used for calculating two different AMFs to determine the vertical columns from the slant columns of the GOME-data: (a) all individual in-situ measured profiles for NO_2 and HCHO and (b) the averaged profile for the campaign for both trace gases were implemented in the radiative transfer model GOMETRAN.

Refering to Fig. 5 the implementation of two different NO_2-profiles in the calculation of AMF leads to differences in tropospheric vertical columns of NO_2 retrieved from GOME-data. Taking into account the measured vertical profile of NO_2 during MINOS (each and the averaged one) a difference of 25% (2.6×10^{14} molec/cm^2) in calculating the tropospheric vertical column of this trace gas can be observed. This value is lower than the uncertainties of the GOME retrievals of tropospheric NO_2 (4.5×10^{14} molec/cm^2) (see Table 2).

The same comparison using different AMFs as described for NO_2 is carried out for the retrieval of the tropospheric vertical columns of HCHO (see Fig. 6). In this case in-situ measured HCHO-profiles (each individual profile and an averaged profile) were implemented in the radiative transfer model. The calculation of the tropospheric vertical column of HCHO using the measured profiles (each profile as well as the averaged profile for the campaign) shows almost no deviation between both results (difference of 1.3×10^{13} molec/cm^2 (~0.5%)) (see Table 2).

For the intercomparison of GOME and in-situ-measurements as well as MATCH-MPIC-model outputs, NO_2 values averaged over 100 m bins were compared. The GOME and in-situ measurements overlap with each other and with the calculated model results during campaign period. Taking into account the error bars of both, the aircraft and the satellite based data, the two instruments agree within their accuracy

ACPD
3, 3051–3094, 2003

limits in most cases (see Fig. 5). That means the discrepancy between GOME and the in-situ-data is in the range of the standard deviation of the in-situ-measurements and the model. Considering the mean values for the MINOS campaign for NO_2, the difference between GOME (using the individual profiles) and in-situ measurements are 3.6×10^{14} molec/cm^2 for the tropopause height of 17 km and 4.6×10^{14} molec/cm^2 for the height of the tropopause of 12 km. The comparision between GOME and MATCH-MPIC yields a deviation of 2.7×10^{14} molec/cm^2 using the simple photochemical equilibrium between NO, NO_2 O_3 and JNO_2. Considering the subtraction of NO from NO_x for the tropopause height of 12 km a deviation of 1.9×10^{14} molec/cm^2 can be obtained. The additional conversion of NO to NO_2 by the peroxy radicals was taken into account in the MATCH-MPIC-simulation to calculate the output of NO_x. Regarding the influence of hydrocarbons in photochemical reactions to produce additional NO_2 the deviation between GOME and the output of model data can be reduced to ~30% using the subtraction of NO_x and NO in contrast to use the simple photochemical equilibrium. The calculated averaged NO_2-profile (see Fig. 3) reflects that the main part of the tropospheric amount (7.1×10^{14} molec/cm^2) is observed in the BL, taken into account the vertical distribution between 0–17 km altitude. The partition of the vertical NO_2-profile in the different atmospheric layers 0–1 km, 1–2 km, 2–3 km, 3–4 km reflects that 68% of tropospheric NO_2 were observed in the lowest atmospheric layer, 11.5% in an altitude between 1–2 km, 5.6% between 2–3 km and 3.3% in an height of 3–4 km of the total column.

Thus the rest of 11.6% of the tropospheric vertical column amount was detected above the 4 km. The calculated mean value of 1.2×10^{15} molec/cm^2 based on GOME data shows that this Nadir-viewing instrument is able to measure the vertical column amount of the BL (considering the use of a modified AMF based on in-situ-data for this campaign).

In Fig. 6 the comparison of the measured and model data is shown for the trace gas HCHO. For this case study the in-situ as well as the MATCH-MPIC-data are averaged in 1 km bins. For the first time a comparison between satellite based GOME

ACPD
3, 3051–3094, 2003

and in-situ airborne measurements was carried out for the trace gas HCHO. During the MINOS campaign the results of both measurement systems agree well for the tropospheric vertical columns of HCHO. That means the discrepancy of the validation of the GOME data and the in-situ measurements is between 1.2×10^{15} molec/cm^2 and 5.6x1015 molec/cm^2 (< 25%) for all comparisons taken into account the individual measured HCHO-profile for the AMF calculation. The discrepancy between the output of the MATCH-MPIC-model and the in-situ measurements is ~30%, and the comparison between GOME and the results of the MATCH-MPIC-data shows a mean deviation of ~17%. In most cases the output of the MATCH-MPIC-model shows lower values for the tropospheric vertical columns of HCHO compared to the measured data (Kormann et al., 2003). The reason for this discrepancy can be an underestimation of the emission of NMHC (non methane hydro carbons) and the fact that the reactions of the terpenes are not explicitly included in the scheme that means the precursors of HCHO in photochemical reactions in the MATCH-MPIC-model are undervalued. The emission of additional CO and acetone instead in the MATCH-MPIC-model leads in this case not to the observed vertical columns of HCHO. The same applies to some higher industrial hydrocarbons: e.g. aromatics and alkenes >C_3 (private communication).

The measured HCHO-profiles show that this trace gas can be observed mainly with a mean value of 5.3×10^{15} molec/cm^2 (=66% of the total tropospheric vertical column based on in-situ measurements) in the lower troposphere (0–4 km). 28.9% can be detected in the lowest atmospheric layer (0–1 km), 17.1% in a height of 1–2 km, 11.5% between 2 and 3 km and 7.5% at 3–4 km altitude. The calculated mean value based on GOME measurements (6.4×10^{15} molec/cm^2) is 20% lower compared to the averaged value of in-situ data during the MINOS campaign in view to the tropospheric vertical column of HCHO. Therefore the GOME results demonstrate its ability to measure tropospheric vertical amounts of HCHO of the free and upper troposphere as well as of the BL.

This can be demonstrated by the investigation of the sensitivity regarding to the density of the radiance I_l measured by GOME. I_l is a function of atmospheric parameters

ACPD
3, 3051–3094, 2003

($p(z)$, which influence the radiative field (e.g. O_3-profile)) and thus a function of height (z), a variable of zenith ($\mu = \cos\theta$) and azimuth (Φ) angle combined in weighting functions $\omega_I(z, \mu, \Phi)$ and described with a Taylor series. These weighting functions are dependent on the "averaged condition of the atmosphere" ($p(z)$), the observing geometry of the instrument and the considered wavelength (λ, for NO_2: 437.5 nm and for HCHO: 346 nm, according to the fitting window of both trace gases). As follows weighting functions describe the induced changes of the incoming radiance in the instrument based on infenitesimal modifications of the parameter p in the height z.

For this study weighting functions $\omega_I(z, \mu, \Phi)$ based on the in-situ measurements of the profiles (ρ) of NO_2 and HCHO were calculated for the MINOS campaign (mean value for SZA = 25°). In the second step the change of the incoming density of radiance (ΔI) was calculated under the condition that the concentrations of the defined trace gas changed ($\Delta\rho$).

$$\Delta I = \frac{\omega_I(z, \mu, \Phi)\Delta\rho}{\rho}. \quad (1)$$

As result modifications concerning the slant columns of NO_2 and HCHO as a function of height were obtained for the defined vertical resolution (for NO_2 100 m, for HCHO 1 km) (see the following equation).

$$\Delta SC = \ln\left(\frac{I_0}{I}\right)\frac{1}{\sigma} \approx -\frac{\Delta I}{I_0}\frac{1}{\sigma}, \quad (2)$$

where I_0 in the approximation is the radiance at the top edge of the atmosphere and σ is the cross section for the appropriate trace gas.

Refering to Fig. 7 a change of the mixing ratio of 1 ppt in 100 m bins for NO_2 yields the highest sensitivity of the GOME measurements at a height of 3 km and a decrease of 37% for the atmospheric layer between 0–3 km. Similar results were obtained for the trace gas HCHO (see Fig. 8). The maximum of the sensitivity is found at an altitude of 4 km and a decrease of 34% can be observed taking into accout the atmospheric layers between the surface and 4 m. For analysing the difference between the mean values

ACPD
3, 3051–3094, 2003

of normal distributed data sets under the condition of the same scattering with respect to the results of the compared systems the t-distribution (T) is used. That means the t-distribution is used instead of normal distribution whenever the standard deviation is estimated (see the following equation, Bronstein, 1979).

$$T = \frac{\overline{X} - \overline{Y}}{\sqrt{(n_1 - 1)S_x^2 + (n_2 - 1)S_y^2}} \sqrt{\frac{n_1 n_2 (n_1 + n_2 - 2)}{n_1 + n_2}}, \quad (3)$$

where n_1, n_2 are the numbers of the analysed data points and S_x^2 and S_y^2 are the empirical variances, with $k = n_1 + n_2 - 2$ (degree of freedom).

Both measurement systems (GOME and in-situ) and the results of MATCH-MPIC for both trace gases NO_2 and HCHO were analysed using the above equation. That means the value of T is a measure of deviation between two samples with a defined degree of freedom. So the significant level can be defined (Sachs, 2000) (see Table 3). On the condition that both measurement systems (GOME – in-situ – measurements) are observing the same air masses the significant level has a value of > 0.5% for the trace gas NO_2. This high significance can be reached in less than 5 of 1000 cases on the basis of systematic measuring errors. The results of both systems show differences which can be considered as correct with a probability of 99.5%. In case of the trace gas HCHO (GOME – in-situ – measurements) the calculation of the significance level with a value around 0.1% reflects that the deviation in the results of both systems can not be explained by statistical errors.

4.2. Transport and build-up of tropospheric trace gases during the MINOS campaign

The measurements of the GOME instrument reveal enhanced tropospheric columns of NO_2 and HCHO (s. Figs. 9 and 10) during the MINOS campaign in the eastern Mediterranean region. For the episode from 1 to 3 August 2001 this study shows an increase of the amount of NO_2 to up to $2.6 \cdot 10^{15}$ molec/cm^2 and of up to $1.1 \cdot 10^{16}$ molec/cm^2 for the HCHO over this region.

From this we conclude that polluted air masses were either transported towards this region or emitted in this region. In order to answer this question backtrajectories have been calculated. All backtrajectories start over Crete at different heights (12 000, 9000, 7000, 5500, 4000, 3000, 2000 and 1000 m) and travel backwards in time for 5 days. Every 6 h (at 00:00, 06:00, 12:00, and 18:00 UT) from 1 to 3 August a new set of backtrajectories was released from the same starting point over Crete. One set contains trajectories being released at 900 to 200 hPa on a 100 hPa altitude grid. Altogether 800 trajectories have been using *Traj.x*, (private communication) a trajectory model developed at IUP-Bremen. For the meteorogical initialisation the ECMWF analysis data which are provided on model levels every 6 h (at 00:00, 60:00, 12:00, and 18:00 UT) are used.

Figure 11 shows the trajectory density of all trajectories arriving over Crete. The trajectory density is derived by projecting all trajectories onto a latitude-longitude grid independent of their current height. Every occurrence of a trajectory within the boundaries of each gridpoint is counted. The figure shows that airmasses arriving at Crete overpass mainly southern central Europe, south eastern Europe and northern Africa. However, the trajectory density in this projection reveals no height information. Figure 14 shows where the trajectories on their way to Crete were at a given date (given in day of year (DoY)). The day of year 208 refers to 27 July and DoY 213 refers to 1 August 2001.

In order to find out whether anthropogenic pollution could have taken place, contacts of the trajectories with the planetary boundary layer are evaluated. The result of this evaluation is displayed in Fig. 12. It gives evidence that polluted air masses being probed over Crete originate mainly from the Black Sea region. The longitude-pressure-projection of the trajectory density suggests that air masses originated above south east Asia are not influenced with anthropogenic pollution (see Fig. 13). Nevertheless strong uplift of air masses from the boundary layer into the free troposphere due to convection can not be regarded in a trajectory calculation. Convection often takes place on horizontal scales of less than 10 km and on time scales of 10 to 20 min. That

ACPD
3, 3051–3094, 2003

means that by a global model (like the ECMWF analysis model) convection is regarded as a parameterized subgrid process (Tiedke, 1989). In order to find out weather air masses being uplifted from the boundary layer by convection into the major trajectory paths the Total Totals Index was calculated for every 6 h in the period from 27 July to 3 August. The Total Totals Index is a simple index derived from the temperature lapse rate between 850 and 500 hPa and from the moisture content at 850 hPa. The likelihood of thunderstorms increases with an increasing Total Totals Index. The risk of severe weather due to atmospheric instability in the US is empirically defined as follows:

As a rule a thumb a Total Totals Index of more than 44 implies convection. Since the index stayed below 44 over south east Asia around 27 July 2001 it indicates that no convection was taking place above this area (see Fig. 15).

As a result the enhanced trajectory analysis reveals no indication for Asian plumes reaching Crete during 1 to 3 August 2001. On the other hand it is likely that boundary layer air was uplifted during the overpass of the trajectories above Europe since the Total Totals Index shows convection above Great Britain and Central Europe on 27 July (see Fig. 15) and the Black Sea Region on 31 July 2001 (see Fig. 16). This explains the elevated CO levels of up to 30 ppb at around 5 km being seen in the MATCH-MPIC-model above Crete indicating the transport of polluted air in this altitude range (see Fig. 17) (Lawrence et al., 2002).

5. Summary

The case studies presented here show a comparison for the trace gas NO_2 and a validation for GOME measurements for HCHO between satellite based measurements and in-situ data. In addition modeled MATCH-MPIC results computed for the MINOS campaign were compared. GOME-pixels along the Falcon track were analysed, in-situ measurements and MATCH-MPIC-profiles were retrieved to obtain the tropospheric amount of NO_2 and HCHO. The GOME-data analysis was optimized by using mea-

ACPD
3, 3051–3094, 2003

sured profiles of the trace gases based on in-situ measurements to calculate the tropospheric AMF. The analysis of profiles based on in-situ measurements showed that the main part of the tropospheric vertical columns of NO_2 and HCHO is present in the BL. By calculating weighting functions based on GOME data and considering in-situ measurements it was demonstrated that the GOME results contain information of vertical tropospheric amount down to the BL.

The results of both measurement systems were found to agree within their accuracy limits even though the tropospheric vertical columns of these trace gases were often near the detection limit of GOME. Consequently the results of the determination of the T-size reflect a high significance level for NO_2 compared to HCHO for this campaign. Case studies in view of transport processes in combination with analyses of back-trajectories reflect that most of the polluted air masses came from the European continent e.g. during the time period of 1 to 3 August 2001. The transport to the atmospheric layer in the 7000 m-level is in this case responsible of the polluted air masses during these days by taking into account meteorological data and in addition the profile of the trace gas CO as an indicator for pollution situations.

Acknowledgements. Parts of this work have been funded by the University of Bremen, Germany, the DLR/DARA, the European Community, and the European Space Agency (ESA). We especially thank the organizers of the MINOS campaign J. Lelieveld, Max-Planck-Institute for Chemistry, Atmospheric Chemistry Department, Mainz, Germany and N. Mihalopoulos, Crete University, Environmental Chemical Processes Laboratory, Department of Chemistry, Greece and the helpful assistance of M. de Reus.

References

Atkinson, R.: Atmospheric chemistry of VOCs and NO_x, Atmos. Environ., 34, 2063–2101, 2000.

Burrows, J. P., Weber, M., Buchwitz, M., Rozanov, V. V., Ladstätter-Weissenmayer, A., Richter, A., de Beek, R., Hoogen, R., Bramstedt, K., Eichmann, K.-U., Eisinger, M., und Perner, D.: The Global Ozone Monitoring Experiment (GOME): Mission Concept and First Scientific Results, J. Atm. Sciences, 56, 151–175, 1999.

Burrows, J. P., Richter, A., Weber, M., Eichmann, K.-U., Bramstedt, K., Ladstätter-Weißenmayer, A., Wittrock, F., Eisinger, M., and Hild, L.: Satellite observations of tropospheric and stratospheric gases, in: Chemistry and Radiation Changes in the Ozone Layer, eds. C. Zerefos et al., 301–329, Kluwer Academic Publisher, 2000.

Bronstein-Semendjajew: Taschenbuch der Mathematik, Verlag H. Deutsch, 1979.

Calvert, J. G. and Stockwell, W. R.: deviations from the O_3-NO-NO_2 photostationary state in tropospheric chemistry, Can. J. Chem., 61, 983–992, 1983.

Chance, K., Palmer, P., Spurr, R. J. D., Martin, R. V., Kurosu, T. P., and Jacob, D. J.: Satellite observations of formaldehyde over North America from GOME, Geophys. Res. Lett., 27, 3461–3464, 2000.

Crawford, J., Davis, D., Chen, G., Bradshaw, J., Sandholm, S., Gregory, G., Sachse, G., Anderson, B., Collins, J., Blake, D., Singh, H., Heikes, B., Talbot, R., and Rodriguez, J.: Photostationary state analysis of the NO_2-NO system based on airborne observations from the western and central North Pacific, J. Geophys. Res., 101, 2053–2072, 1996.

Fishman, J., Watson, C. E., Larsen, J. C., and Logan, J. A.: The distribution of tropospheric ozone determined from satellite data, J. Geophys. Res., 95, 3599–3617, 1990.

Hauser, C.: Charakterisierung eines Messsystems zur Bestimmung der NO_2-Photolysefrequenz in der Troposphäre – Labormessungen und Flugzeugmessungen, Diplomarbeit, Fachhochschule München, DLR, Oberpfaffenhofen, 2002.

Heland, J., Schlager, H., Richter, A., and Burrows, J.: First comparison of tropospheric NO_2 column densities retrieved from GOME measurements and in situ aircraft profile measurements, Geophys. Res. Lett., 29, 2, 44-1–44-4, 2002.

Junkermann, W., Platt, U., and Volz-Thomas, A.: A Photoelectric Detector for the Measurement of Photolysis Frequencies of Ozone and Other Atmospheric Molecules, J. Atmos. Chem., 8, 203–227, 1989.

Kelly, T. J. and Fortune, C. R.: Continuous monitoring of gaseous formaldehyde using an improved fluorescence approach, Int. J. Env. Anal. Chem., 54, 249–263, 1994.

Kormann, R., Fischer, H., de Reus, M., Lawrence, M. G., Brühl, Ch., von Kuhlmann, R., Holzinger, R., Williams, J., Lelieveld, J., Warneke, C., de Gouw, J., Heland, J., Ziereis, H., and Schlager, H.: Formaldehyde over the Eastern Mediterranean during MINOS: Comparison of Airborne In-situ Measurements With 3-D-Model Results, Atmos. Chem. Phys. Discuss., 3, 1303–1331, 2003

Ladstätter-Weissenmayer, A., Burrows, J. P., and Perner, D.: Biomass burning over Indonesia

as observed by GOME, Earth Obs. Quart. 58, 28–29, 1998.
Lawrence, M. G. , Crutzen, P. J., Rasch, P. J., Eaton, B. E., and Mahowald, N. M.: A model for studies of tropospheric photochemistry: Description, global distributions and evaluation, J. Geophys. Res., 104, 26 245–26 277, 1999.
Lawrence, M. G., Rasch, P. J., von Kuhlmann, R., Williams, J., Fischer, H., de Reus, M., Lelieveld, J., Crutzen, P. J., Schultz, M., Stier, P., Huntrieser, H., Heland, J., Stohl, A., Forster, C., Ebern, H., Jakobs, H., and Dickerson, R. R.: Global chemical weather forcasts for field campaign planning: predictions and observations of larger-scale features during MINOS, CONTRACE, and INDOEX, Atmos. Chem. Phys. Discuss., 2, 1545–1597, 2002.
Leue, C., Wenig, M., Wagner, T., Platt, U., and Jähne, B.: Quantitative analysis of NO_x emissions from GOME satellite image sequences, J. Geophys. Res., 106, 5493–5505, 2001.
Levine, J. S.: Global biomass burning: Atmospheric, climatic and biospheric implications, Global biomass burning, Atmospheric, climatic, and biospheric implications edited by Levine, 1991.
Macdonald, A. M., Wiebe, H. A., Li, S. M., Dryfhout-Clark, H., Asalian, K., Lu, G., Wang, D., Schiller, C. L., Harris, G. W., Sumner, A. L., and Shepson, P. B.: Results of a formaldehyde intercomparison study in Ontario, Atmospheric Environment Service, Ontario, Canada, 1999.
Nash, T.: The colorimetric estimation of formaldehyde by means of the Hantzsch reaction, Biochemistry, 55, 416–421, 1953.
Olivier, J. G. J., Bouwman, A. F. van der Maas, C. W. M., Berdowski, J. J. M., Veldt, C., Bloos, J. P. J., Visschededijk, A. J. J., Zandveld, P. Y. J., and Haverlag, J. L.: Description of EDGAR Version 2.0: A set of global inventories of greenhouse gases and ozone-depleting substances for all anthropogenic and most natural sources on a per country $1^\circ \times 1^\circ$ grid. RIVM Rep, 771060002, Rijksinstituut, Bilthoven, The Netherlands, 1996.
Palmer, P. I., Jacob, D. J., Fiore, A. M., Martin, R. V., Chance, K., and Kurosu, T. P.: Mapping isoprene emissions over North America using formaldehyde columns observations from space, J. Geophys. Res., 101, 2053–2072, 2002.
Richter, A. and Burrows, J. P.: Retrieval of tropospheric NO_2 from GOME measurements, Adv. Space Res., 29, 11, 1673–1683, 2002.
Rozanov, V., Diebel, D., Spurr, R. J., and Burrows, J. P.: GOMETRAN: A radiative transfer model for the satellite project GOME – the plane parallel version, J. Geophys. Res., 102, 16 683–16 695, 1997.
Sachs, L.: Angewandte Statistik, Springer-Verlag, 2000.

ACPD
3, 3051–3094, 2003

Sander, S. P., Friedl, R. R., DeMore, W. B., Golden, D. M., Kolb, C. E., Kurylo, M. J., Hampson, R. F., Huie, R. E., Molina, M. J., and Moortgat, G. K.: Chemical Kinetics and Photochemical Data for Use in Stratospheric Modeling, Supplement to Evaluation 12: Update of Key Reactions, JPL Publication 00-3, NASA Panel for Data Evaluation, Evaluation Number 13, 8 March 2000, Jet Propulsion Laboratory, Pasadena, California, 2000.

Shimizu, A., and Tsuda, T.: Variations in tropical tropopause observed with radiosondes in Indonesia, Geophys. Res. Lett, 27, 16, 2541–2544, 2000.

Tiedke, M.: A Comprehensive Mass Flux Scheme for Cumulus Parameterization in Large Scale Models, Monthly Weather Review, August 1989.

Volz-Thomas, A., Lerner, A., Pätz, H. W., Schulz, M., McKenna, D. S., Schmitt, R., Madronich, S., and Röth, E. P.: "Airborne measurements of the photolysis frequency of NO_2", J. Geophys. Res., 101, 18 613–18 627, 1996.

Von Kuhlmann, R.: Tropospheric photochemistry of O_3, its precursors and the hydroxyl radical: A 3D modeling study considering Non-Methane hydrocarbons, PhD Thesis, University of Mainz, Germany, 2001a.

Von Kuhlmann, R.: Tropospheric Photochemistry of Ozone, its Precursors and the Hydroxyl Radical: A3D-Modeling Study Considering Non-Methane Hydrocarbons, PhD-Thesis, Johannes-Gutenberg-Universität Mainz, Mainz, Germany, 2001b.

Von Kuhlmann, R., Lawrence, M. G., Crutzen, P. J., and Rasch, P. J.: A Model for Studies of Tropospheric Ozone and Non-Methane Hydrocarbons: Model Description and Ozone Results, J. Geophys. Res., 108, D9, DOI10.1029/2002JD002893, 2003.

Wagner, V., v. Glasow, R., Fischer, H., and Crutzen, P. J.: Are CH_2O measurements in the Marine boundary layer suitable for testing the current understanding of CH_4 photooxidation?, A model study, J. Geophys. Res., 107, 10 1029–10 1043, 2002.

Ziereis, H, Schlager, H., Schulte, P., Köhler, I., Marquardt, R., and Feigl, C.: In situ measurements of the NO_x distribution and variability over the eastern North Atlantic, J. Geophys. Res., 104, 16 021–16 032, 1999.

Ziereis, H., Schlager, H., Schulte, P., v. Velthoven, P. F. J., and Slemr, F.: Distributions of NO, NO_x, and NO_y in the upper troposphere and lower stratosphere between 28° and 61° N during POLINAT 2, J. Geophys. Res., 105, 3653–3664, 2000.

ACPD

3, 3051–3094, 2003

Table 1. Contribution of possible error sources in GOME analysis to the uncertainty of the retrieved troposperic NO_2 and HCHO columns

Error source	Uncertainty (NO_2)	Uncertainty (HCHO)
Fitting error	5%	50%
Stratospheric subtraction	0.5×10^{15} molec/cm^2	–
NO_2 – HCHO vertical profile assumption (AMF)	50%	50%
Aerosol assumption (AMF)	35%	35%
Surface albedo assumption (AMF)	max. 50%	max. 50%
Cloud effects	30%	30%

ACPD
3, 3051–3094, 2003

Table 2. Comparision for different AMF for the calculation of tropospheric vertical columns of NO_2 and HCHO

	Mean value of NO_2 [molec/cm^2]	Mean value of HCHO [molec/cm^2]
Implementation of each profile	1.2×10^{15}	6.3×10^{15}
Implementation of an averaged profile for the campaign	8.7×10^{14}	6.4×10^{15}

ACPD
3, 3051–3094, 2003

Table 3. Calculation of the t-distribution with a degree of freedom of 10 for the trace gases NO_2 and a degree of freedom of 8 for HCHO

	T (with k = 10 for NO_2 and k = 8 for HCHO)	Significant level
NO_2 GOME – in-situ	3.23	> 0.5%
NO_2 GOME – MATCH-MPIC	4.05	> 0.5%
HCHO GOME – in-situ	0.75	< 0.1%
HCHO GOME – MATCH-MPIC	0.65	< 0.1%

ACPD
3, 3051–3094, 2003

Table 4. Classification of weather phenomenon based on the Total Totals Index in view to analyse the influence of convection

Total Totals Index	Weather phenomenon
44–45	Isolated moderate thunderstorms
46–47	Scattered moderate/few heavy thunderstorms
48–49	Scattered moderate/few heavy/isolated severe thunderstorms
50–51	Scattered heavy/few severe thunderstorms and isolated tornadoes
52–55	Scattered to numerous heavy/few to scattered severe thunderstorms/few tornadoes
> 55	Numerous heavy/scattered severe thunderstorms and scattered tornadoes

ACPD
3, 3051–3094, 2003

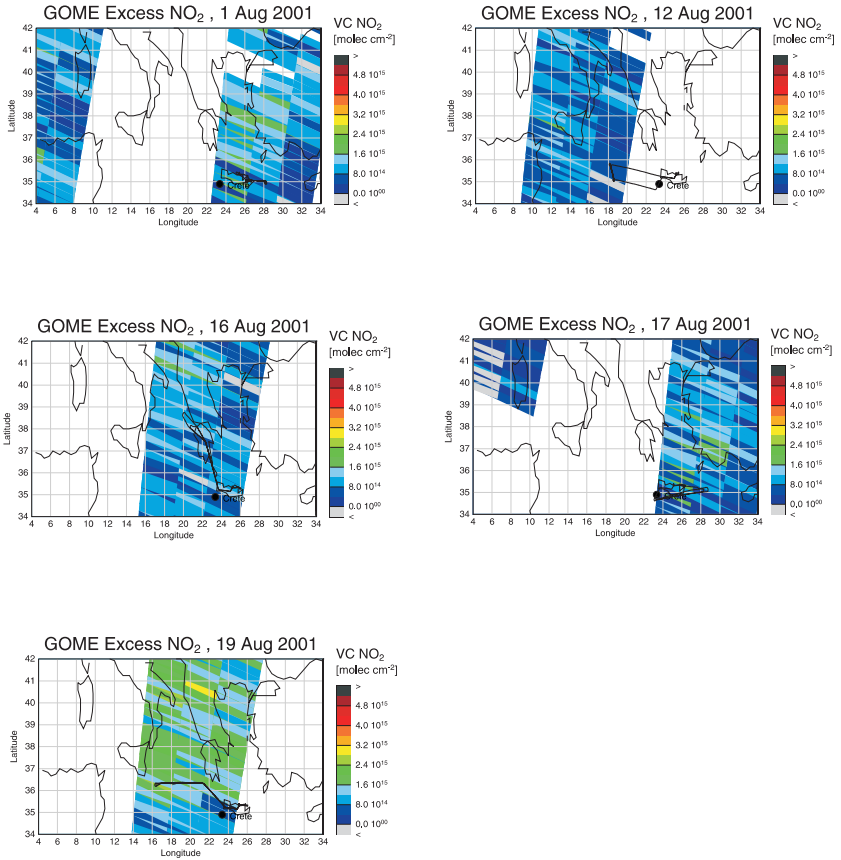

Fig. 1. (a) Vertical tropospheric columns of NO_2 along a Falcon track on the days of overflights of GOME during the MINOS campaign.

ACPD
3, 3051–3094, 2003

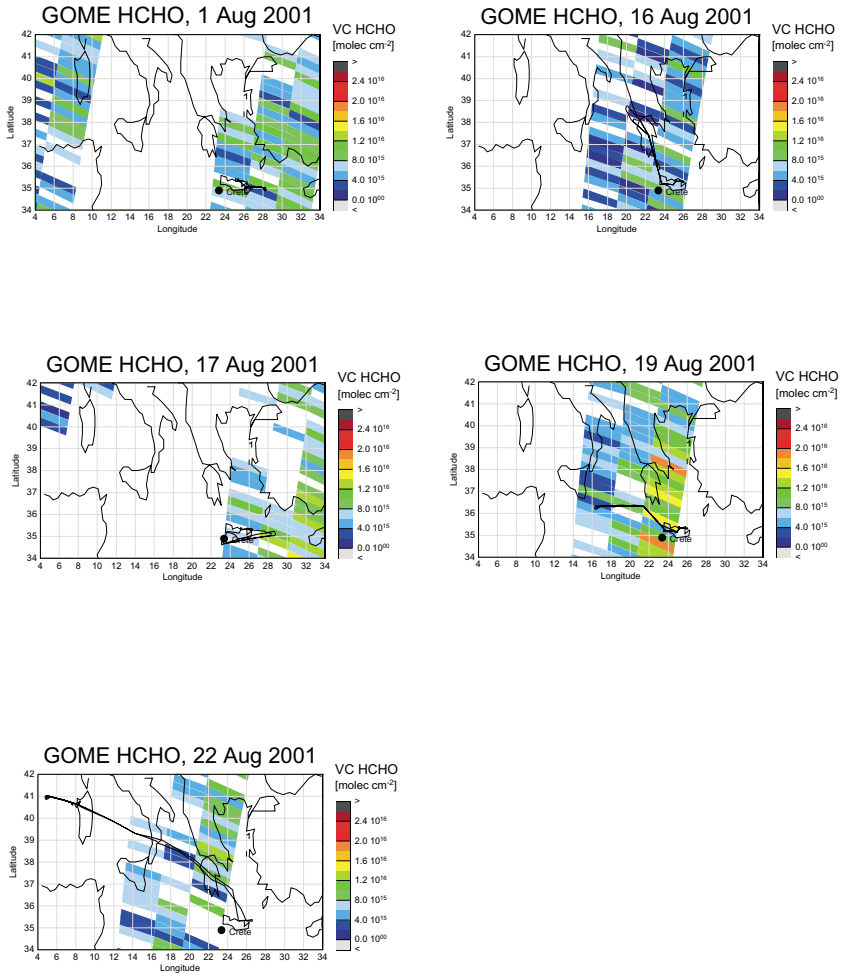

Fig. 1. (b) Vertical tropospheric columns of HCHO along a Falcon track on the days of overflights of GOME during the MINOS campaign.

ACPD
3, 3051–3094, 2003

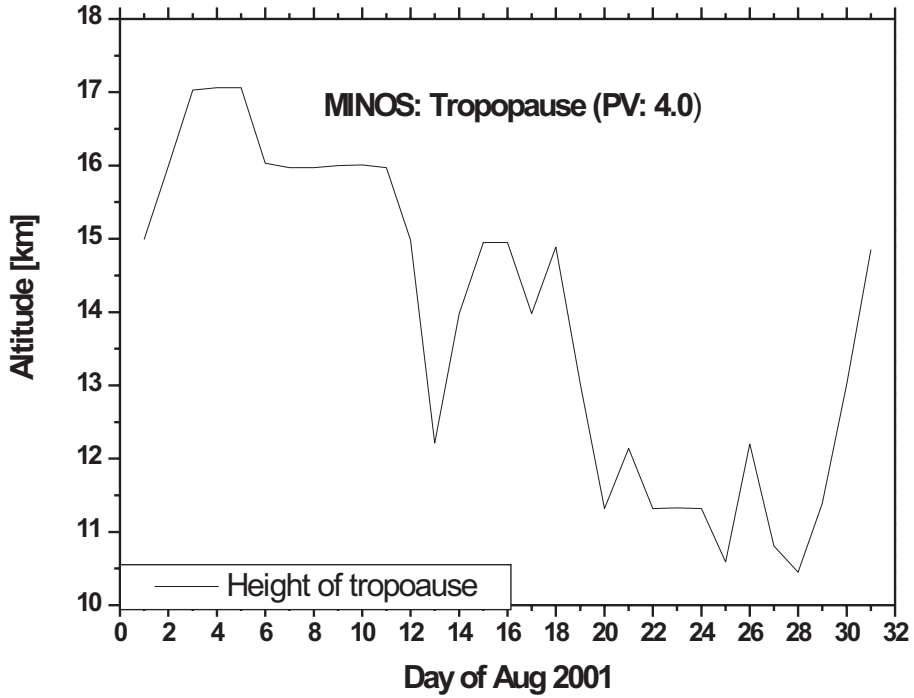

Fig. 2. The height of the tropopause is defined to be at the altitude of 4 PV-Units over Crete-during the MINOS campaign in August 2001.

ACPD
3, 3051–3094, 2003

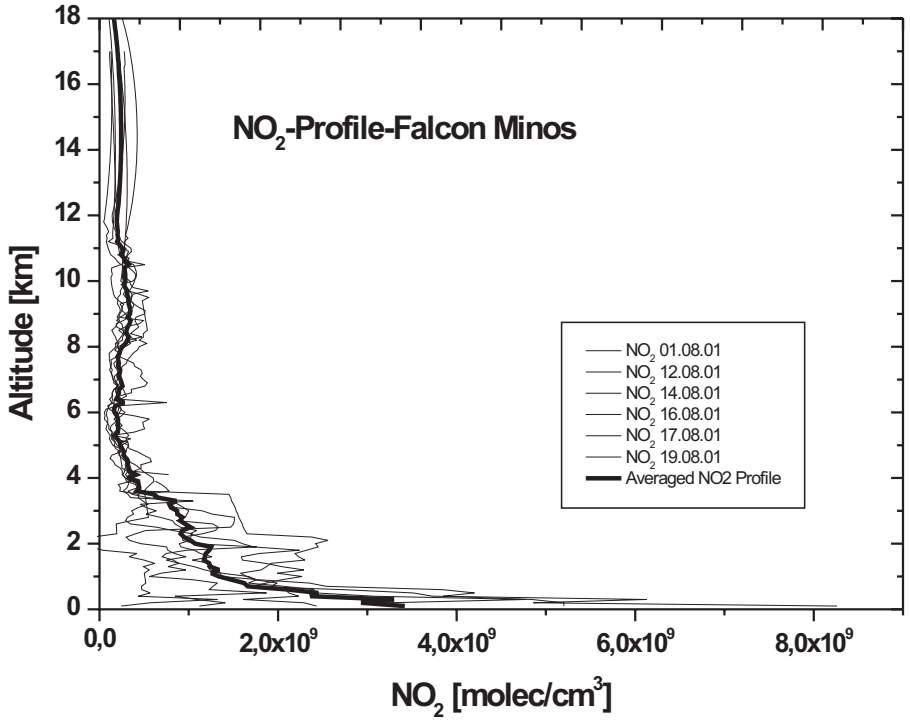

Fig. 3. Vertical profiles of NO_2 and the calculated averaged profile based on in situ-measurements detected during the MINOS campaign in July and August 2001.

ACPD
3, 3051–3094, 2003

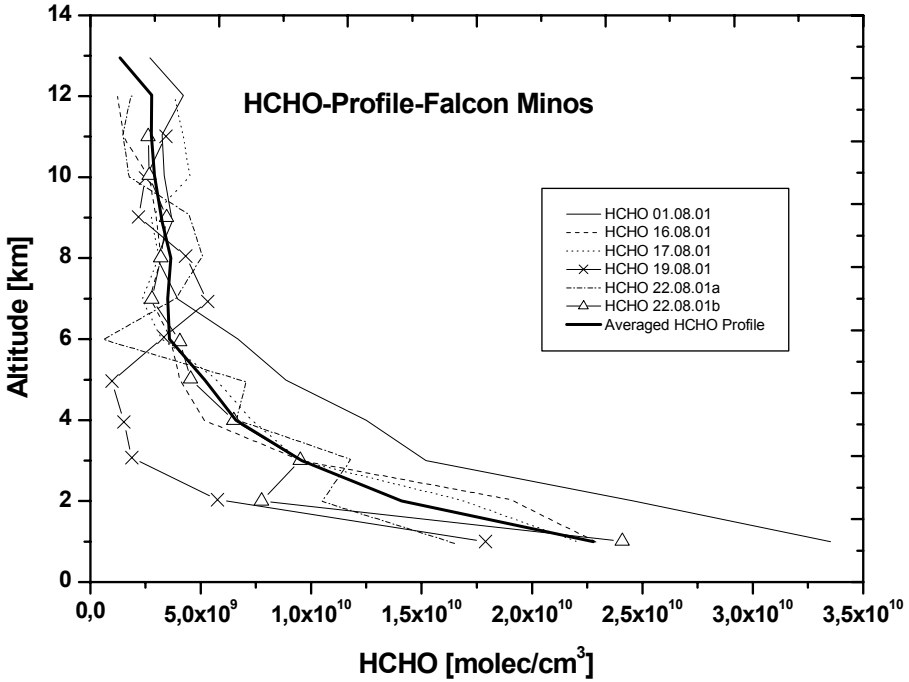

Fig. 4. Vertical profiles of HCHO and the calculated averaged profile based on in situ-measurements detected during the MINOS campaign in July and August 2001.

ACPD
3, 3051–3094, 2003

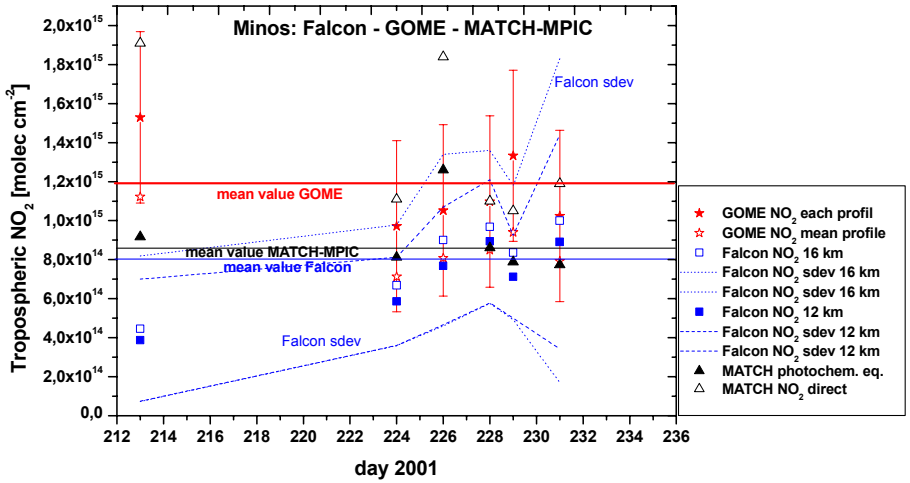

Fig. 5. Comparisons of measurements of tropospheric vertical column densities of NO_2 (100 m bins for NO_2), based on in-situ-measurements and on GOME data acquired during the MINOS campaign in July and August 2001. In addition calculated MATCH-MPIC-model data are also shown considering the same bin-averaging as for the in-situ measurements.

ACPD
3, 3051–3094, 2003

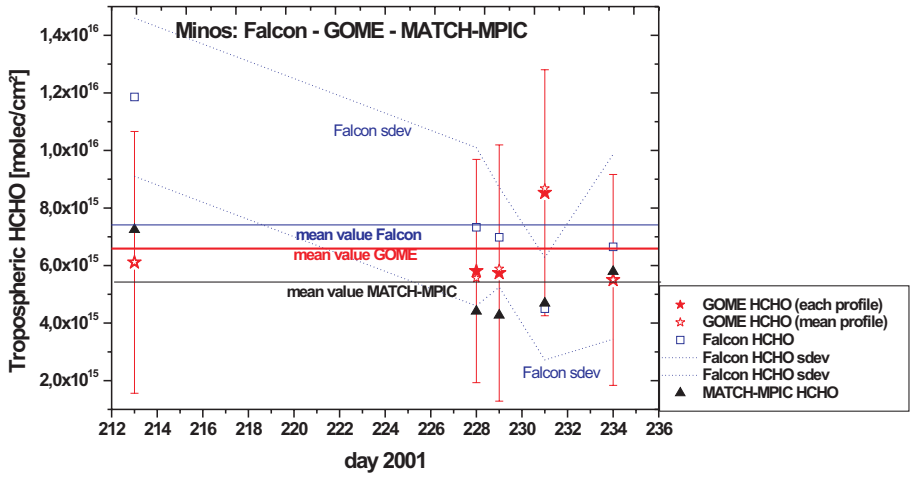

Fig. 6. Comparisons of measurements of tropospheric vertical column densities of HCHO based on in-situ-measurements (for HCHO 1 km bins) and on GOME data acquired during the MINOS campaign in July and August 2001. In addition calculated MATCH-MPIC-model data are also shown considering the same bin-averaging as for the in-situ measurements.

ACPD
3, 3051–3094, 2003

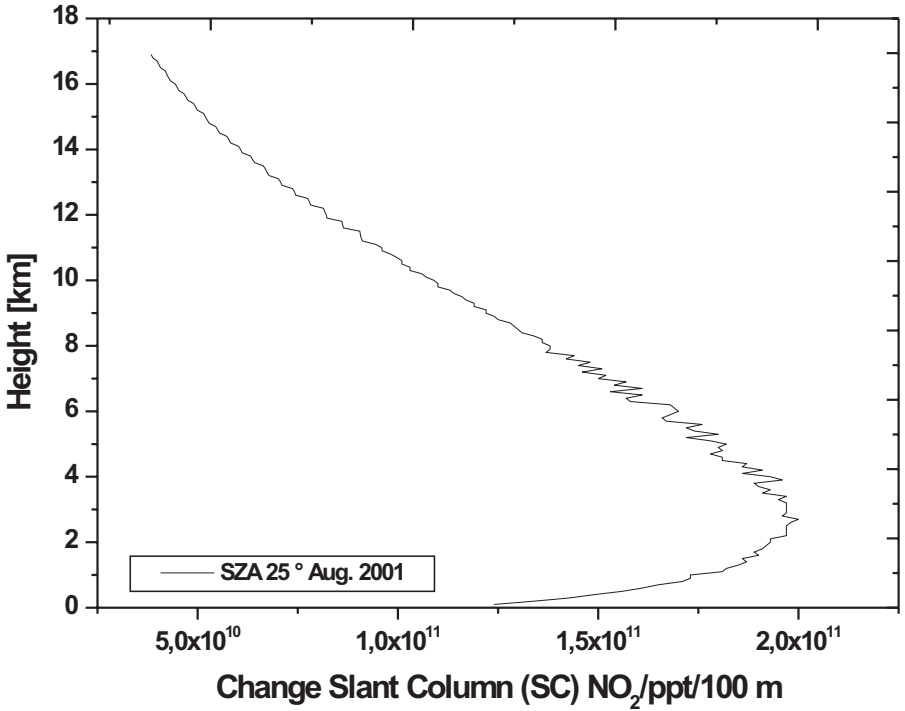

Fig. 7. Analysis of the sensitivity studies based on in-situ data of NO_2 with respect to the changes in slant columns as a function of height for GOME measurements.

ACPD
3, 3051–3094, 2003

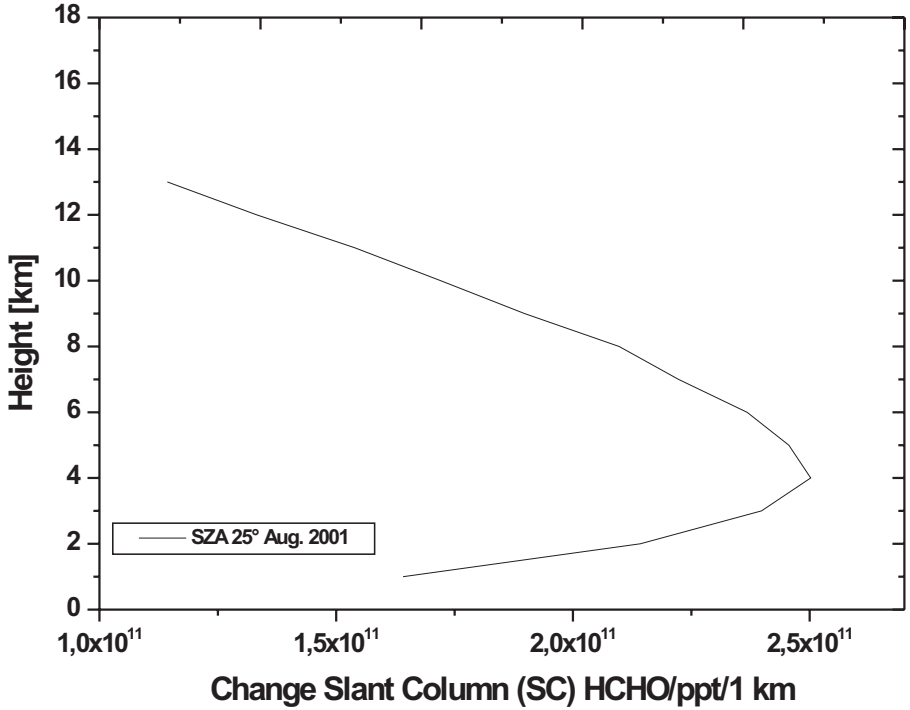

Fig. 8. Analysis of the sensitivity studies based on in-situ data of HCHO with respect to the changes in slant columns as a function of height for GOME measurements.

ACPD
3, 3051–3094, 2003

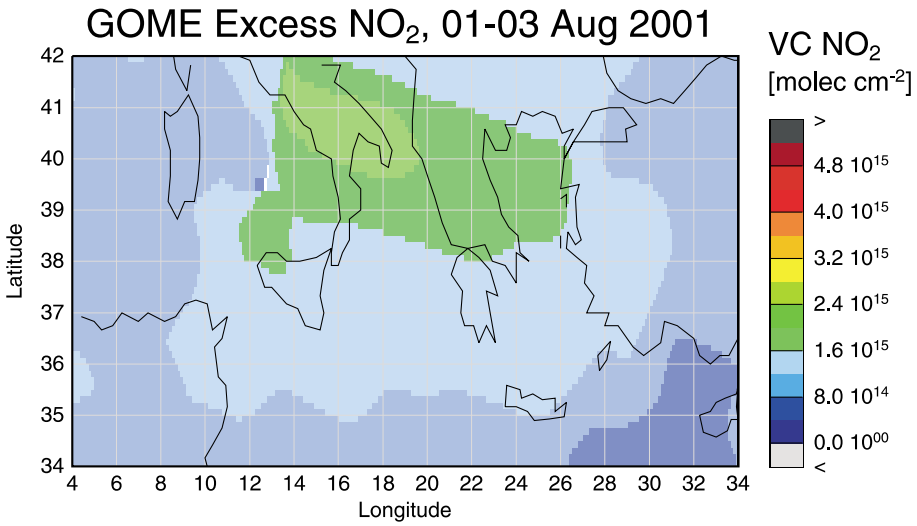

Fig. 9. Global GOME measurements of tropospheric NO_2 amounts in the time period of 1 to 3 August 2001 analysed for the Mediterranean region during the MINOS campaign.

ACPD
3, 3051–3094, 2003

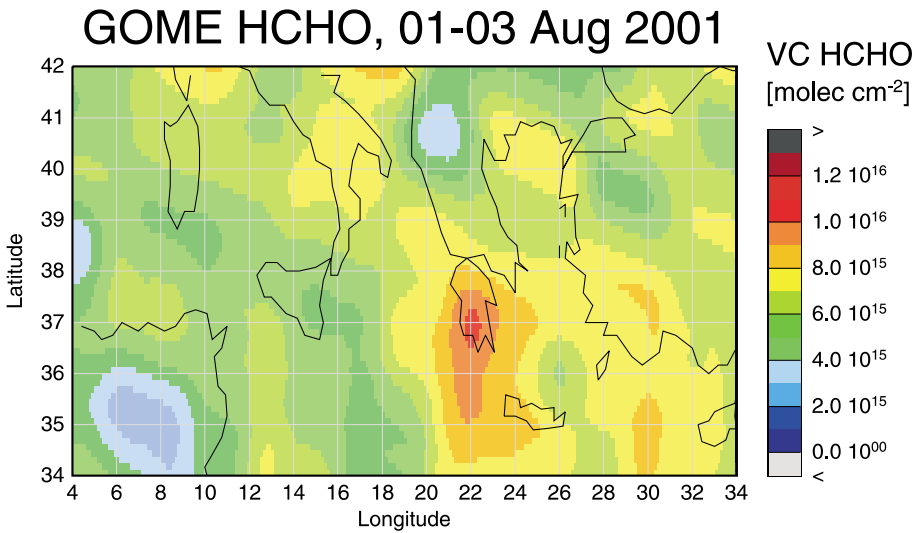

Fig. 10. Global GOME measurements of tropospheric HCHO amounts in the time period of 1 to 3 August 2001 analysed for the Mediterranean region during the MINOS campaign.

ACPD
3, 3051–3094, 2003

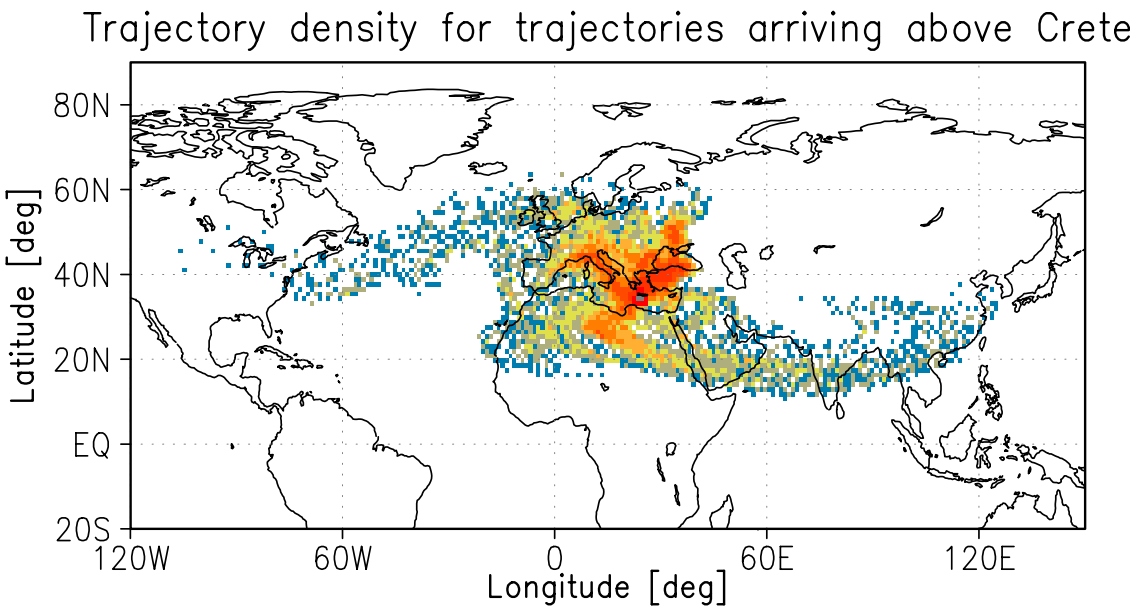

Fig. 11. Trajectory density for trajectories arriving at Crete during 1 and 3 August 2001. The trajectory density is derived by projecting all trajectories overpassing a certain location at any given height to the ground. Trajectories on all height levels are weighted equally. So this figure reveals no height information. The trajectory density is given in an arbitrary colorscale. It is shown that air masses arriving at Crete overpass mainly southern central Europe, south eastern Europe and northern Africa.

ACPD
3, 3051–3094, 2003

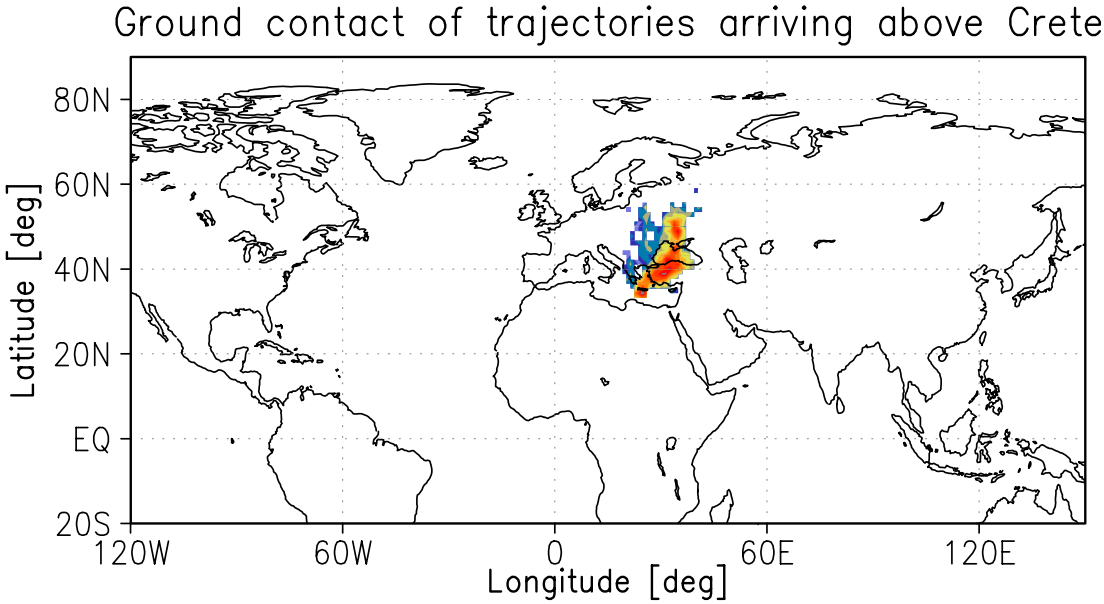

Fig. 12. Ground contact of trajectories arriving at Crete during 1 and 3 August 2001. A ground contact occurs when a trajectory drops below an altitude of 2000 m above ground. The number of ground contacts are also given in an arbitrary colorscale. This map reveals that most of the pollution detected at Crete originates from the Black Sea area. An arbitrary colorscale is used. Red indictes a high number of contacts to the planetary boundary layer, blue a smaller amount of contacts.

ACPD
3, 3051–3094, 2003

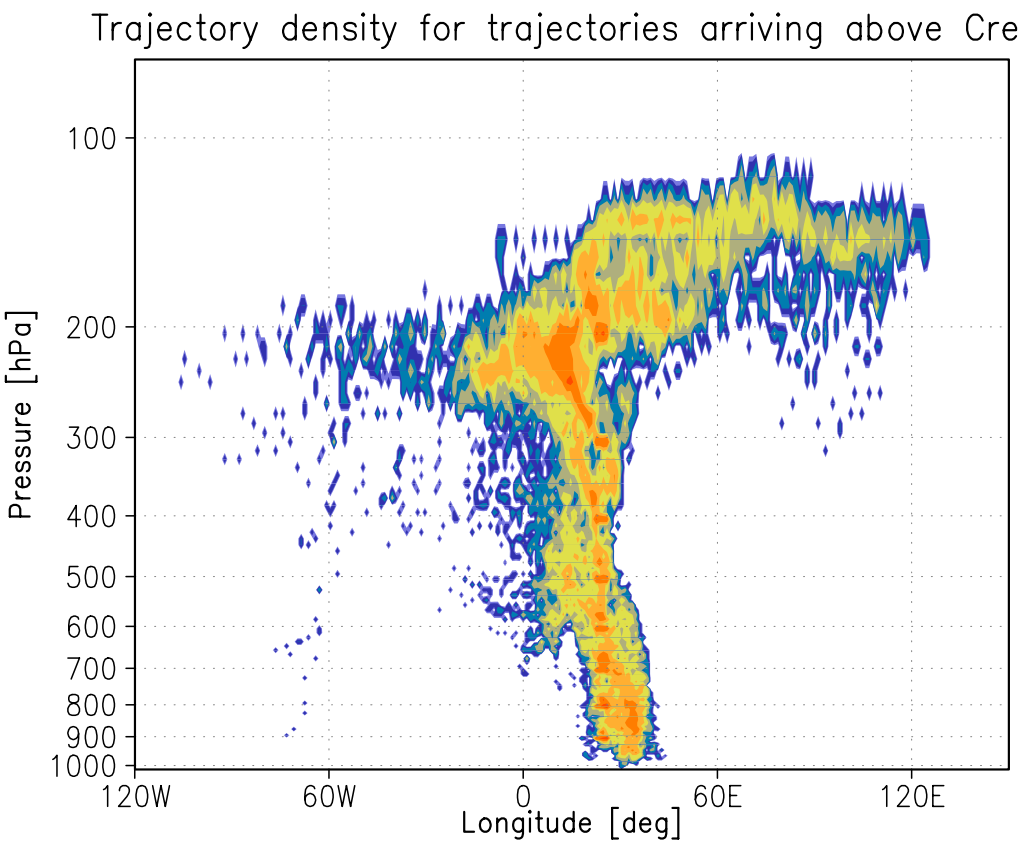

Fig. 13. Longitude-pressure projection of the trajectory density of all trajectories arriving over Crete on 1 to 3 August 2001. This projection reveals that trajectories originated above south-east-Asia had are hardly impacted by anthropogenic pollution. For this graph an arbitrary colorscale is used.

ACPD
3, 3051–3094, 2003

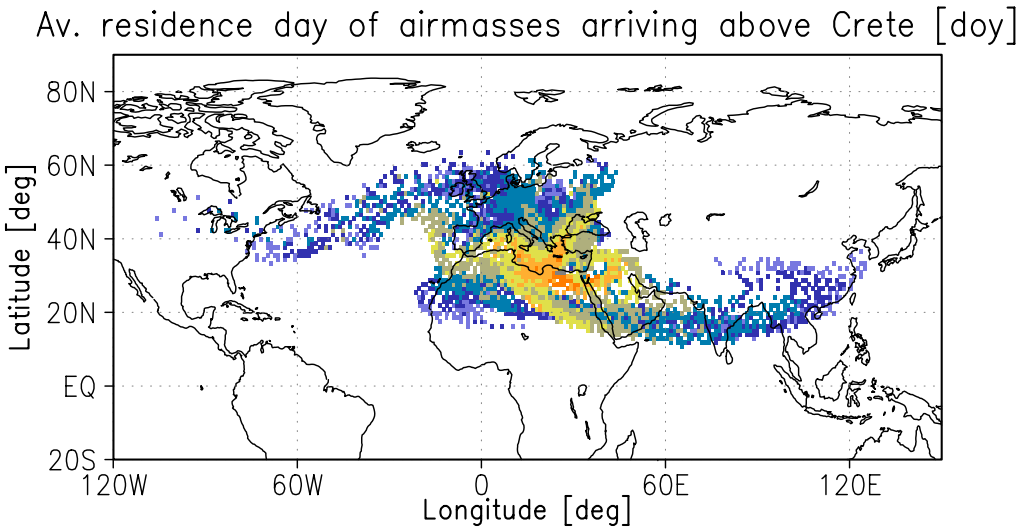

Fig. 14. Averaged date of the trajectories' occurrence at a distinct location (given as day of the year (DoY)). DoY 208 refers to 27 July 2001, DoY 213 refers to 1 August 2001 and DoY 215 refers to 3 August 2001. Trajectories started around DoY 208 and 209 above south east Asia, northern Atlantic, north western Europe and western Africa in order to arrive above Crete on 1 to 3 August 2001. All times within each column are averaged to get one value per gridcell. So the values close the arrival point should not be taken into account.

ACPD
3, 3051–3094, 2003

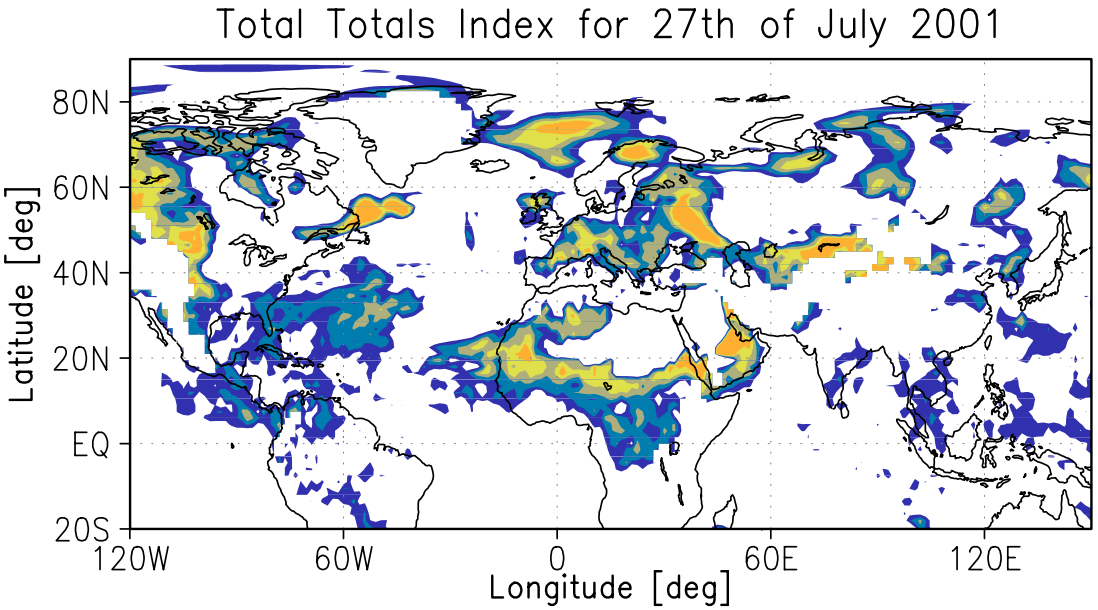

Fig. 15. Total Totals Index for 27 July. It shows thunderstorm activity above Europe but hardly any activity above south east Asia.

ACPD
3, 3051–3094, 2003

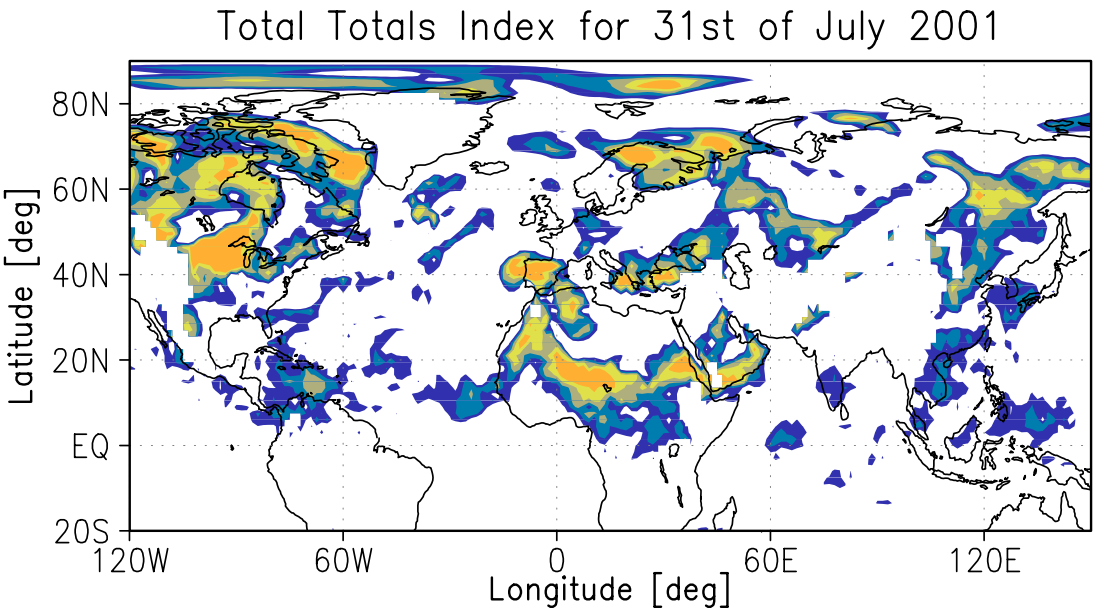

Fig. 16. Total Totals Index for 31 July. It shows thunderstorm activity above the Black Sea region and in the north eastern region of the Mediterianien Sea. This may cause uplifting of anthropogenically polluted air from the boundary layer into the free troposphere.

ACPD
3, 3051–3094, 2003

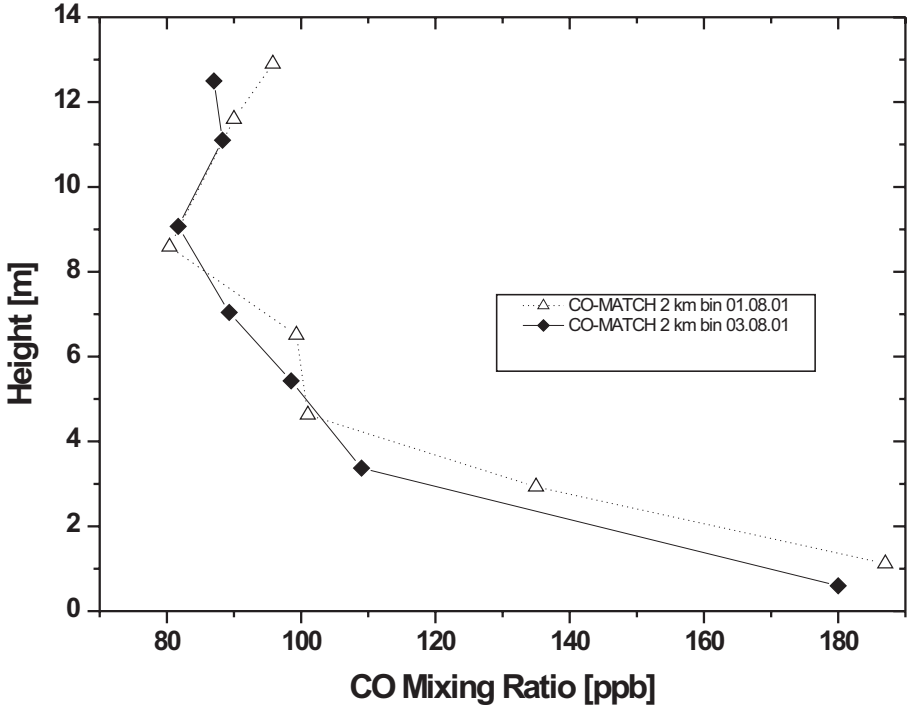

Fig. 17. Vertical profiles of the trace gas CO for 1 and 3 August 2001 calculated along the Falcon track with the MATCH-MPIC-model.

ACPD
3, 3051–3094, 2003